

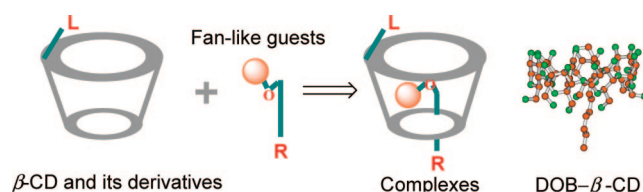
## A Comparative Study on the Binding Behaviors of $\beta$ -Cyclodextrin and Its Two Derivatives to Four Fanlike Organic Guests

Le Xin Song,<sup>\*,†</sup> Hai Ming Wang,<sup>†</sup> Xue Qing Guo,<sup>‡</sup> and Lei Bai<sup>†</sup>

Department of Chemistry and Department of Polymer Science and Engineering, University of Science and Technology of China, Hefei, 230026 Anhui, China

solexin@ustc.edu.cn

Received July 7, 2008



Four fanlike organic compounds, 1-ethoxybenzene (EOB), 1-butoxybenzene (BOB), 1-dodecyloxybenzene (DOB), and 1-(dodecyloxy)-2-methoxybenzene (DOMB), were chosen as guests, and  $\beta$ -cyclodextrin ( $\beta$ -CD) and its two derivatives, mono(2-*O*-2-methyl)- $\beta$ -CD and mono(2-*O*-2-hydroxy-propyl)- $\beta$ -CD, were chosen as hosts. Energy changes involved in host–guest inclusion processes were clearly obtained by applying semiempirical PM3 calculations. According to this, probable structures of the host–guest inclusion complexes were proposed. The inclusion systems in aqueous solution were investigated by UV–vis spectroscopy and nuclear magnetic resonance (<sup>1</sup>H NMR) titration, and the formation constants (*K*) of the inclusion complexes were determined using the Benesi–Hildebrand equation. Moreover, two solid inclusion complexes of  $\beta$ -CD with EOB and DOB were prepared and characterized by Fourier transform infrared spectra, X-ray powder diffraction, <sup>1</sup>H NMR, electrospray ionization mass spectrometry, and thermogravimetric analyses. Results showed that the host–guest stoichiometries in the inclusion complexes were all 1:1 both in solid state and in aqueous solution. As for the same host, the values of *K* increased in the order EOB < BOB < DOB, in strong association with the fan handle in the fanlike molecules; that is to say, the *K* values increased with increasing carbon chain length of substituent on benzene ring. In addition, the *K* values of DOMB complexes were larger than those of DOB complexes for the same CD, indicating that the introduction of an extra *o*-methoxyl group on DOB further stabilized the CD inclusion complexes. The decomposition activation energies of EOB– $\beta$ -CD and DOB– $\beta$ -CD were very similar but significantly larger than that of free  $\beta$ -CD.

### Introduction

Cyclodextrins (CDs) are  $\alpha$ -1,4-linked cyclic oligomers of D-glucopyranose that possess the remarkable property to form inclusion complexes with a wide variety of guests.<sup>1–3</sup>  $\beta$ -CD, one of the most common CDs, has the shape of a hollow truncated cone with 14 secondary hydroxy groups around the larger circumference of the cavity and 7 primary hydroxy groups around the smaller opening. Mono(2-*O*-2-methyl)- $\beta$ -CD (M $\beta$ -CD) and mono(2-*O*-2-hydroxypropyl)- $\beta$ -CD (HP $\beta$ -CD) are two

simple derivatives of  $\beta$ -CD, in which the 2-OH group of one of seven glucose units of  $\beta$ -CD is substituted by a methoxy group or a hydroxypropyloxy group, respectively (Figure 1).

There are many theoretical and experimental studies on the stoichiometries, structures, and stabilities of the supramolecular inclusion complexes of CDs with guest molecules in solution,<sup>4–6</sup> as well as a number of investigations on the preparations and characterizations of solid CD inclusion complexes.<sup>7–9</sup> It is found that the stoichiometries and stabilities of CD inclusion com-

<sup>†</sup> Department of Chemistry.

<sup>‡</sup> Department of Polymer Science and Engineering.

(1) Liu, Y.; Yang, Y. W.; Yang, E. C.; Guan, X. D. *J. Org. Chem.* **2004**, *69*, 6590–6602.

(2) Muller, A.; Wenz, G. *Chem.–Eur. J.* **2007**, *13*, 2218–2223.

(3) Szejtli, J. *Chem. Rev.* **1998**, *98*, 1743–1753.

(4) Bea, I.; Gotsev, M. G.; Ivanov, P. M.; Jaime, C.; Kollman, P. A. *J. Org. Chem.* **2006**, *71*, 2056–2063.

(5) Wenz, G.; Han, B. H.; Muller, A. *Chem. Rev.* **2006**, *106*, 782–817.

(6) Liu, Y.; Han, B. H.; Zhang, H. Y. *Curr. Org. Chem.* **2004**, *8*, 35–46.

(7) Giordano, F.; Novak, C.; Moyano, J. R. *Thermochim. Acta* **2001**, *380*, 123–151.

(8) Harata, K. *Chem. Rev.* **1998**, *98*, 1803–1827.

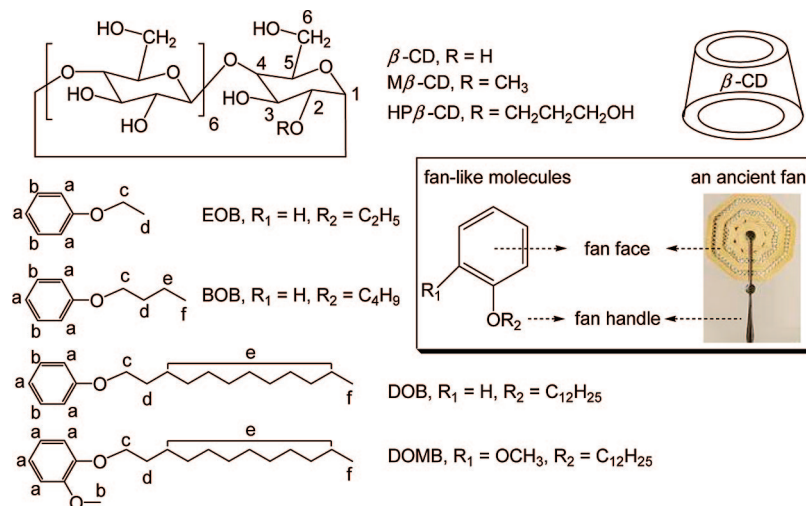


**FIGURE 1.** Structural features of  $\beta$ -CD, its two derivatives, and four fanlike guest molecules.

plexes, both in aqueous solution and in solid state, vary markedly with the shape, volume, and polarity of organic guest molecules.<sup>10–12</sup> There are many reports on the inclusion systems between CDs and aliphatic or aromatic organic guests.<sup>13–15</sup> However, few efforts have been made to evaluate the relationship between aromatic ring and aliphatic chain in CD inclusion complexes of fan-shaped guest molecules. Moreover, the investigation on the influence of the structural differences among a set of similar guest molecules on the properties of CD inclusion complexes, such as the interaction energy, preparation analysis, spectral property, thermal behavior, and decomposition kinetics, is important and significant not only in academic studies but also in industrial applications.

According to these views, four organic compounds, 1-ethoxybenzene (EOB), 1-butoxybenzene (BOB), 1-dodecyloxybenzene (DOB), and 1-(dodecyloxy)-2-methoxybenzene (DOMB), are chosen as guests, and  $\beta$ -CD, M $\beta$ -CD, and HP $\beta$ -CD are chosen as hosts. It should be noted that EOB, BOB, and DOB not only possess a rigid benzene-ring backbone but also have a flexible aliphatic side chain structure with different lengths linked directly to a carbon atom of the benzene ring (Figure 1). DOMB is a simple derivative of DOB, in which one H atom of the benzene ring in the *ortho* position of the ether oxygen bond is substituted with a methoxyl group. The structural frame of an ancient fan widely used in old China, which is made up of a fan face and a fan handle, is shown in Figure 1. The fanlike guest molecules in the manuscript are composed of two parts, benzene ring and side chain. The benzene ring is somewhat like the fan face, and the side chain on the benzene ring looks like the fan handle.

First, the formation processes of the inclusion complexes of  $\beta$ -CD and its two derivatives with the four fanlike organic guests

in water are examined using a semiempirical PM3 method in order to obtain information about the formation, structures, and stabilities of the 12 CD inclusion complexes.

Second, the binding behaviors of CDs to the guests in the 12 inclusion systems are investigated in detail by UV–vis spectrophotometry and <sup>1</sup>H NMR titration methods. Many reports have confirmed that some cyclic aromatic guests like a fan face, either without a handle such as benzene<sup>13</sup> or with a very short fan handle such as phenol,<sup>13</sup> do not interact strongly with CDs. Our aim was to examine the relationship between the side chain length of the substituent on the aromatic ring of guests and the binding abilities of CDs to the guests. In other words, this work focused on evaluating the effect of the side chain as a fan handle on the stabilities of inclusion complexes based on theoretical and experimental studies.

Third, significant efforts have been dedicated to the comparison in preparation, spectral property, and thermal decomposition kinetics between the CD inclusion complexes of similar structural units, i.e., EOB and DOB.

We believe that a comprehensive insight into the influence of the competitive complexation of side chain and benzene ring in a guest molecule with CDs on the formations, stoichiometries, stabilities, and decomposition behaviors of CD complexes will facilitate understanding of the nature of inclusion phenomena between CDs and guests.

## Results and Discussion

**Differences in the Values of  $\Delta E_c$ ,  $\Delta E_f$ , and  $\Delta E_i$  of Different Inclusion Complexes.** The inclusion complexations between CDs and the fanlike guests in water were investigated using the PM3 method<sup>16</sup> in the present work. The calculated values of  $\Delta E_c$ ,  $\Delta E_f$ , and  $\Delta E_i$  of 12 CD inclusion complexes in water, as well as the values of the distances (*Z*) between the center of the cavities of CDs and the ether oxygen atoms of the guest molecules, are listed in Table 1. Although two different starting geometries were considered in the formation of an inclusion complex, only the lowest  $\Delta E_i$  value of the inclusion complex is given in Table 1. Similarly, only the geometry at the lowest calculated  $\Delta E_i$  value is regarded as the optimized complex geometry of the inclusion complex. The values of *Z*

(9) Song, L. X.; Wang, H. M.; Yang, Y.; Xu, P. *Bull. Chem. Soc. Jpn.* **2007**, *80*, 2185–2195.

(10) Kano, K.; Hasegawa, H. *J. Am. Chem. Soc.* **2001**, *123*, 10616–10627.

(11) Braga, S. S.; Goncalves, I. S.; Herdtweck, E.; Teixeira-Dias, J. J. C. *New J. Chem.* **2003**, *27*, 597–601.

(12) Liu, Y.; Cao, R.; Chen, Y.; He, J. Y. *J. Phys. Chem. B* **2008**, *112*, 1445–1450.

(13) (a) Rekharsky, M. V.; Inoue, Y. *Chem. Rev.* **1998**, *98*, 1875–1917. (b) Bertrand, G. L.; Han, S. M.; Armstrong, D. W. *J. Phys. Chem.* **1989**, *93*, 6863–6867.

(14) Rodriguez-Llamazares, S.; Yutronic, N.; Jara, P.; Englert, U.; Noyong, M.; Simon, U. *Eur. J. Org. Chem.* **2007**, 4298–4300.

(15) Liu, Y.; Fan, Z.; Zhang, H. Y.; Yang, Y. W.; Ding, F.; Liu, S. X.; Wu, X.; Wada, T.; Inoue, Y. *J. Org. Chem.* **2003**, *68*, 8345–8352.

(16) Stewart, J. J. P. *J. Comput. Chem.* **1989**, *10*, 209–220.

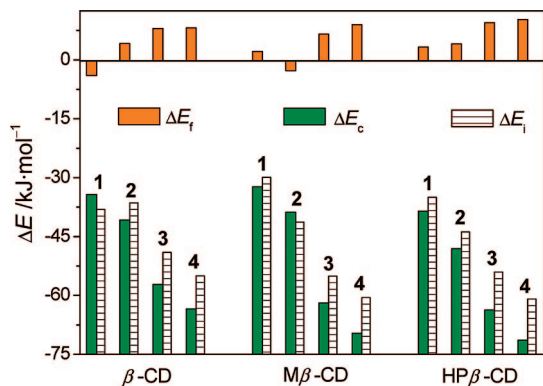


**FIGURE 2.**  $\Delta E_f$ ,  $\Delta E_c$ , and  $\Delta E_i$  values of the inclusion complexes of  $\beta$ -CD,  $M\beta$ -CD, and  $HP\beta$ -CD with EOB 1, BOB 2, DOB 3, and DOMB 4 in water.

**TABLE 1.**  $\Delta E_c$ ,  $\Delta E_f$ , and  $\Delta E_i$  in  $\text{kJ}\cdot\text{mol}^{-1}$  of 12 Host–Guest Inclusion Complexes in Water

inclusion complex	$\Delta E_c$	$\Delta E_f$	$\Delta E_i$	Z (pm)
EOB– $\beta$ -CD	–34.3	–3.8	–38.1	300
BOB– $\beta$ -CD	–40.8	4.4	–36.4	300
DOB– $\beta$ -CD	–57.2	8.2	–49.0	200
DOMB– $\beta$ -CD	–63.4	8.4	–55.0	0
EOB– $M\beta$ -CD	–32.3	2.4	–29.9	400
BOB– $M\beta$ -CD	–38.8	–2.5	–41.3	300
DOB– $M\beta$ -CD	–61.9	6.8	–55.1	0
DOMB– $M\beta$ -CD	–69.7	9.2	–60.5	100
EOB– $HP\beta$ -CD	–38.5	3.5	–35.0	200
BOB– $HP\beta$ -CD	–48.1	4.3	–43.8	300
DOB– $HP\beta$ -CD	–63.7	9.7	–54.0	0
DOMB– $HP\beta$ -CD	–71.4	10.5	–60.9	0

were obtained corresponding to the lowest  $\Delta E_i$  values in the inclusion systems.

As shown in Table 1, the sufficiently large negative values of  $\Delta E_i$  ranging from  $-60.9$  to  $-29.9 \text{ kJ}\cdot\text{mol}^{-1}$  clearly reveal that the formations of the 12 inclusion complexes are all energetically favorable. In other words, the complexes can be thermodynamically stable in water, since the  $\Delta E_i$  values are a reflection of the degree of stability of the complexes.<sup>17</sup>

Figure 2 shows that there are very small absolute values of  $\Delta E_f$  on the upper side of the figure as compared with the values of  $\Delta E_c$  or  $\Delta E_i$  on the lower side of the figure for the inclusion complexes. As can be directly seen in Table 1, the values of  $\Delta E_f$  are in the narrow range from  $-3.8$  to  $10.5 \text{ kJ}\cdot\text{mol}^{-1}$ .

With the exception of two inclusion systems, i.e., EOB– $\beta$ -CD ( $-3.8 \text{ kJ}\cdot\text{mol}^{-1}$ ) and BOB– $M\beta$ -CD ( $-2.5 \text{ kJ}\cdot\text{mol}^{-1}$ ), the other 10 systems show positive  $\Delta E_f$  values, suggesting that the deformation behaviors of CD and guest in these systems give a negative contribution to the formations and stabilities of the 10 inclusion complexes. Interestingly, the values of  $\Delta E_f$  appear to increase in the approximate order EOB < BOB < DOB < DOMB for the same CD. This result can be attributed to the increase of flexibility of the carbon chains with the increase of the chain length of the alkoxy groups in the guest molecules.

Further, the bar graph of  $\Delta E_i$  in Figure 2 seems to have a trend similar to that of  $\Delta E_c$  for the 12 inclusion complexes. Clearly, the stabilities of the inclusion complexes increase in the following sequence: EOB < BOB < DOB < DOMB for the same CD.

**Inclusion Complexation Processes and Proposed Intermolecular Interaction Modes.** Figure 3 illustrates the details of the inclusion complexation processes of DOB and DOMB with

$\beta$ -CD in water. As can be seen in Figure 3A, DOB– $\beta$ -CD has the most negative value of  $\Delta E_i$  near the wider rim of  $\beta$ -CD cavity, i.e.,  $Z = 200 \text{ pm}$ ,  $\Delta E_i = -49.0 \text{ kJ}\cdot\text{mol}^{-1}$ .

Figure 3B shows that the inclusion system of DOMB with  $\beta$ -CD has the most negative value of  $\Delta E_i$  just in the center of the cavity of  $\beta$ -CD, i.e.,  $Z = 0 \text{ pm}$ ,  $\Delta E_i = -55.0 \text{ kJ}\cdot\text{mol}^{-1}$ .

The highly negative values of  $\Delta E_i$  of the two inclusion complexes predict that both DOB and DOMB can form stable complexes with  $\beta$ -CD in water. The big difference in the values of Z or  $\Delta E_i$  between the two inclusion complexes of  $\beta$ -CD is ascribed to the contribution of a single *o*-methoxy group. These observations indicate that the introduction of an *o*-methoxy group on the DOB molecule promotes the inclusion complexation between host and guest and further stabilizes the inclusion complex.

The PM3 optimized structures of DOB– $\beta$ -CD and DOMB– $\beta$ -CD in water are schematically illustrated in Figure 4. From Figure 4A and C, it is apparent that no intermolecular hydrogen bonds form between the guest molecules and the OH groups of  $\beta$ -CD in the optimized structures of the two inclusion complexes. Moreover, the side view of DOMB– $\beta$ -CD in Figure 4D displays that the benzene ring in the DOMB molecule is partly included into the inner cavity of  $\beta$ -CD, while the carbon chain on the benzene ring exposes itself to the outside of the cavity from the narrower opening. However, the side view of DOB– $\beta$ -CD in Figure 4B shows that the benzene ring in DOB is not almost included in the cavity of  $\beta$ -CD, while five of 12 carbon atoms on the ether oxygen chain penetrate into the cavity. The findings imply that the inner cavity of  $\beta$ -CD does not bear a structurally selective character with respect to the benzene ring of a guest with a long carbon chain.

In order to further evaluate the effect of the flexibility of the long carbon chain to the inclusion complexations between hosts and guests, a new starting geometry is considered, i.e., when a guest molecule is inserted into the cavity of  $\beta$ -CD, its long carbon chain is assumed to be in a folded position. Based on the starting geometry, the values of  $\Delta E_c$ ,  $\Delta E_f$ , and  $\Delta E_i$  of the inclusion complexes of the four fanlike guests with CDs in water are determined and listed in Table 2.

A remarkable difference between the data in Table 1 and Table 2 is that the values of Z are quite different from each other between the long carbon chain in the guests in an extended position and a folded position. For instance, there are 100 pm of  $|\Delta Z|$  for the complex of  $\beta$ -CD with DOB and 300–400 pm of  $|\Delta Z|$  for the complexes of the two  $\beta$ -CD derivatives with DOB.

Similarly, a large energy difference ( $|\Delta\Delta E| > 9 \text{ kJ}\cdot\text{mol}^{-1}$ ) in  $\Delta E_c$  or  $\Delta E_i$  between the data in Table 1 and Table 2 has been observed for the complexes of CDs with DOB. These results show that modifying the long carbon chain in DOB from an extended to a folded position leads to a positive contribution to the inclusion complexation between DOB and  $\beta$ -CD or its two simple derivatives.

Figure 5 displays the PM3 optimized structure of DOB– $\beta$ -CD in water when the long carbon chain in DOB is in a folded position. Likewise, there are no intermolecular hydrogen bonds between DOB and  $\beta$ -CD (see Figure 5A). Accordingly, it is reasonable that the formation of DOB– $\beta$ -CD is mainly driven by van der Waals force and hydrophobic interaction.

(17) Song, L. X.; Wang, H. M.; Xu, P.; Zhang, Z. Q.; Liu, Q. Q. *Bull. Chem. Soc. Jpn.* **2007**, *80*, 2313–2322.



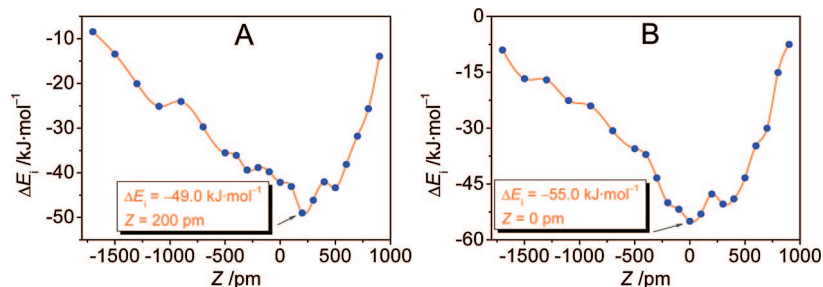


FIGURE 3. Curves of  $\Delta E_i$  versus  $Z$  during inclusion complexation: (A) DOB- $\beta$ -CD and (B) DOMB- $\beta$ -CD systems.

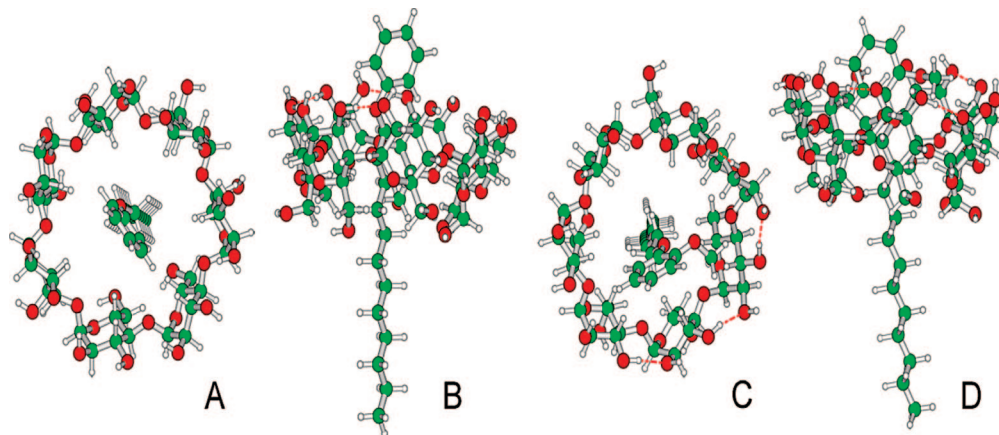


FIGURE 4. Optimized structures of DOB- $\beta$ -CD and DOMB- $\beta$ -CD: top view (A) and side view (B) of DOB- $\beta$ -CD; top view (C) and side view (D) of DOMB- $\beta$ -CD when the long carbon chain in DOB or DOMB is in an extended position.

TABLE 2.  $\Delta E_c$ ,  $\Delta E_f$ , and  $\Delta E_i$  in  $\text{kJ}\cdot\text{mol}^{-1}$  of EOB, BOB, DOB, and DOMB Complexes of CDs in Water<sup>a</sup>

inclusion complex	$\Delta E_c$	$\Delta E_f$	$\Delta E_i$	$Z$ (pm)
EOB- $\beta$ -CD	-34.6	4.2	-30.4	500
BOB- $\beta$ -CD	-44.4	4.8	-39.6	200
DOB- $\beta$ -CD	-74.3	7.9	-66.4	300
DOMB- $\beta$ -CD	-74.8	9.7	-65.1	300
EOB-M $\beta$ -CD	-38.1	3.7	-34.4	300
BOB-M $\beta$ -CD	-47.3	4.9	-42.4	400
DOB-M $\beta$ -CD	-72.6	8.5	-64.1	400
DOMB-M $\beta$ -CD	-80.6	11.4	-69.2	400
EOB-HP $\beta$ -CD	-40.2	4.0	-36.2	300
BOB-HP $\beta$ -CD	-42.7	-3.4	-46.1	300
DOB-HP $\beta$ -CD	-76.0	8.8	-67.2	300
DOMB-HP $\beta$ -CD	-75.9	10.1	-65.8	400

<sup>a</sup> According to the starting geometry in which the long carbon chain of DOB and DOMB is assumed to be in a folded position.

The side view of DOB- $\beta$ -CD in Figure 5B indicates that the benzene ring in DOB is fully included into the cavity of  $\beta$ -CD, whereas nine of 12 carbon atoms on the ether oxygen chain also have been accommodated in the cavity. This configuration implies that there is a close distance between the carbon or hydrogen atoms on the benzene ring and on the ether oxygen chain of DOB in DOB- $\beta$ -CD. Since the arrangement of DOB- $\beta$ -CD has an advantage ( $\Delta\Delta E_i$ ,  $-17.4 \text{ kJ}\cdot\text{mol}^{-1}$ ) in the energy of formation in comparison with the other arrangement, i.e., the long carbon chain of DOB in an extended position, we believe that there may be an interaction between the benzene ring and carbon chain of DOB in DOB- $\beta$ -CD. Nevertheless, further and more detailed evidence is necessary to provide solid proof that the benzene ring and carbon chain of DOB are simultaneously accommodated in the cavity of  $\beta$ -CD.

Similar phenomena also occur in the inclusion systems of  $\beta$ -CD and its two derivatives with EOB, BOB, and DOMB (see Table

2) in the present study. Consequently, analyses and experiments are performed to gain further insight into the inclusion behaviors of the hosts and guests, including the formation, stoichiometries, structures, and stabilities of the inclusion complexes of the CDs with the fanlike guest molecules.

**Direct Evidence of Intermolecular Interaction between the Four Fanlike Guests and  $\beta$ -CD from  $^1\text{H}$  NMR Titrations.** Different chemical shift changes ( $\Delta\delta$ ) of the protons on the benzene ring (H-a), methoxy group (H-b), methylene (H-c, H-d, and H-e), and end methyl group (H-f) in DOMB with increasing molar fractions of DOMB in mixed solutions of  $\beta$ -CD and DOMB are clearly observed during  $^1\text{H}$  NMR titration experiments (Figure 6A).

Further, a bigger decrease of the chemical shift ( $\delta$ ) values for H-3 and H-5 protons of  $\beta$ -CD than those for H-2 and H-4 protons with an increase in the relative concentration of DOMB is observed in Figure 6B.

These phenomena can be attributed to the formation of the inclusion complex of DOMB with  $\beta$ -CD because the H-3 and H-5 protons are inside the cavity of  $\beta$ -CD.

Upon complexation, the protons of the methoxy group in DOMB are affected most, next the benzene ring protons, then the methylene protons, and finally the protons of the end methyl group located at the end of the carbon chain. This observation strongly suggests that the benzene ring of DOMB as well as the methoxy group in the benzene ring is likely to be deeply embedded into the cavity of  $\beta$ -CD, and there is a relatively weak interaction between  $\beta$ -CD and the long carbon chain of DOMB especially the end of the long chain.

According to Figure 6B, the maximum  $\Delta\delta$  values of the H-3 and H-5 protons of  $\beta$ -CD after complexation with DOMB are  $-0.042$  and  $-0.069$  ppm, respectively. The considerably large

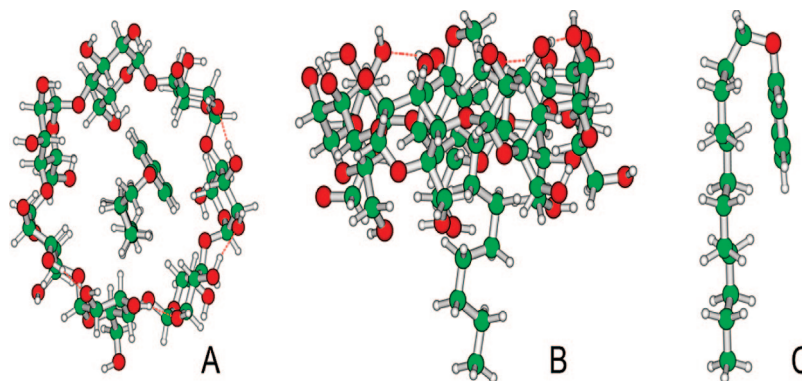


**FIGURE 5.** PM3 optimized structure of DOB- $\beta$ -CD: top view (A) and side view (B) in water according to the starting geometry in which the long carbon chain of DOB is assumed to be in a folded position. (C) DOB at the geometry in the optimized complex.

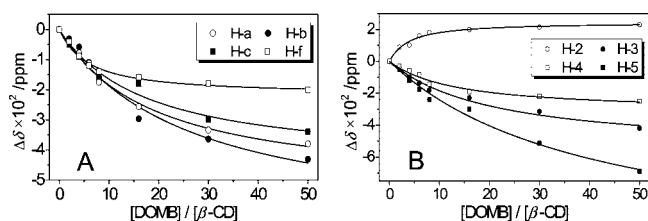


**FIGURE 6.** Plots of  $\Delta\delta$  values of protons of DOB (A) and  $\beta$ -CD (B) versus the concentration ratios of DOB to  $\beta$ -CD.

**TABLE 3.** Maximum  $\Delta\delta$  Values of Protons of EOB, BOB, DOB, DOB, and  $\beta$ -CD upon Complexation

proton	$\Delta\delta_{\beta\text{-CD}}$			
	EOB	BOB	DOB	DOMB
H-a	0.037	-0.043	-0.035	-0.038
H-b	0.046	-0.049	-0.040	-0.043
H-c	0.028	-0.037	-0.030	-0.034
H-d	-0.020	-0.036	-0.027	-0.036
H-e		0.011	-0.025	-0.023
H-f		0.008	0.018	-0.020

proton	$\beta$ -CD			
	$\Delta\delta_{\text{EOB}}$	$\Delta\delta_{\text{BOB}}$	$\Delta\delta_{\text{DOB}}$	$\Delta\delta_{\text{DOMB}}$
H-1	0.012	0.016	0.016	0.017
H-2	0.024	0.027	0.023	0.023
H-3	-0.041	-0.048	-0.042	-0.042
H-4	0.027	-0.014	-0.027	-0.025
H-5	-0.035	-0.041	-0.047	-0.069
H-6	0.021	0.015	0.013	0.019

upfield shifts of both H-3 and H-5 can be explained by the ring current effect of the benzene ring of DOB.<sup>18,19</sup>

In addition, the  $\Delta\delta$  value of the H-5 protons is larger than that of the H-3 protons under different concentrations of DOB. This may be because there is a relatively strong interaction between the H-5 protons of  $\beta$ -CD and the benzene ring of DOB.

Similar phenomena also occur in the inclusion systems of  $\beta$ -CD with EOB, BOB, and DOB (see Table 3) in this study. Hence, the results from NMR titrations provide a direct evidence for the formation of the inclusion complexes of  $\beta$ -CD with the four fanlike guests.

**Formations and Stoichiometries of the Inclusion Complexes of CDs with the Fanlike Guests in Solution.** Typical UV-vis absorption spectra of BOB and DOB upon addition of  $\beta$ -CD in aqueous solution at 298 K are shown in Figure 7A and B, respectively.

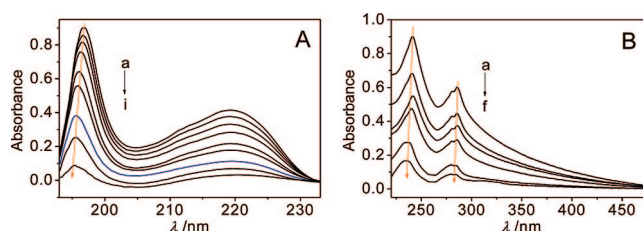


**FIGURE 7.** UV-vis spectra of (A) BOB and (B) DOB ( $5.0 \times 10^{-5} \text{ mol} \cdot \text{dm}^{-3}$ ). The concentrations of  $\beta$ -CD are in the range from 0.0 to  $5.0 \times 10^{-3} \text{ mol} \cdot \text{dm}^{-3}$ .

The absorption spectrum of free BOB shows a narrow band and a broad band with the maximum at about 196.7 and 219.8 nm, respectively. Interestingly, the narrow band at 196.7 nm shifts gradually to the blue, and the intensity of the band decreases with increasing concentration of  $\beta$ -CD. These changes indicate that BOB is experiencing a less polar environment in the case of increasing concentration of  $\beta$ -CD. Considering that the cavity of  $\beta$ -CD is a less polar microenvironment than aqueous solution, the absorption result suggests the formation of  $\beta$ -CD inclusion complex of BOB from water to the cavity.<sup>20</sup>

In the case of the system of DOB with  $\beta$ -CD, similar phenomena have been observed from Figure 7B. For example, the absorption intensity (A) of DOB after complexation with  $\beta$ -CD decreases with increasing concentration of  $\beta$ -CD, and the two peaks at 241.6 and 285.5 nm shift to 234.0 and 283.1 nm, respectively, with the addition of  $\beta$ -CD. Furthermore, similar phenomena are also observed in all other 10 inclusion systems, thereby confirming that there exists an intermolecular interaction between CDs and the fanlike guests.

The constitutions of the inclusion complexes are determined to be 1:1 by means of the continuous variation method (Job's plot).<sup>21,22</sup> The plots describing the interactions between four fanlike guests and  $\beta$ -CD are representatively shown in Figure 8.

Figure 8 depicts the changes ( $\Delta A$ ) in the absorption of the four fanlike guests with increasing the concentration of  $\beta$ -CD

(18) Funasaki, N.; Yamaguchi, H.; Ishikawa, S.; Neya, S. *J. Phys. Chem. B* **2001**, *105*, 760–765.

(19) Yoshikiyo, K.; Matsui, Y.; Yamamoto, T.; Okabe, Y. *Bull. Chem. Soc. Jpn.* **2007**, *80*, 1124–1128.

(20) (a) Song, L. X.; Wang, H. M.; Yang, Y. *Acta Chim. Sinica* **2007**, *65*, 1593–1599. (b) Wagner, D. B.; Stojanovic, N.; Leclair, G.; Jankowski, C. K. *J. Inclusion Phenom. Macrocyclic Chem.* **2003**, *45*, 275–283.

(21) Bardelang, D.; Rockenbauer, A.; Karoui, H.; Finet, J. P.; Tordo, P. *J. Phys. Chem. B* **2005**, *109*, 10521–10530.

(22) Tilloy, S.; Crownin, G.; Monflier, E.; van Leeuwen, P. W. N. M.; Reek, J. N. H. *New J. Chem.* **2006**, *30*, 377–383.

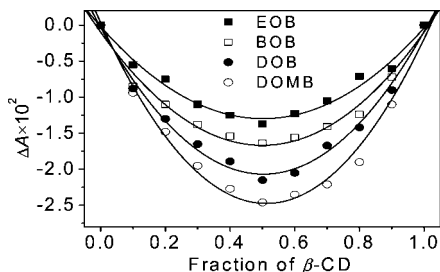


**FIGURE 8.** Equimolar Job's plots for binding of  $\beta$ -CD to four fanlike guests at 298 K in water solutions with  $[\text{guest}] + [\beta\text{-CD}] = 1.0 \times 10^{-4} \text{ mol}\cdot\text{dm}^{-3}$ .

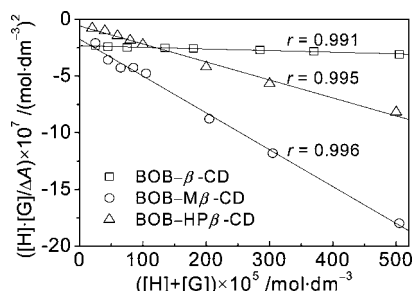


**FIGURE 9.** Plots of  $([\text{CD}]\cdot[\text{BOB}])/\Delta A$  versus  $([\text{CD}] + [\text{BOB}])$ .

where the total concentration of  $\beta$ -CD and guest is kept constant of  $1.0 \times 10^{-4} \text{ mol}\cdot\text{dm}^{-3}$ . The four experimental curves go through maximum values at a molar fraction of 0.5, indicating a 1:1 stoichiometry of the inclusion complexes. Similar phenomena occur also in the inclusion systems of  $\beta$ -CD derivatives and the fanlike guests. Therefore, the intermolecular interactions between CDs (H) and the guests (G) can be represented by eq 1:



where HG represents an inclusion complex formed between H and G.

**K Values and Stability Comparison of the Inclusion Complexes in Solution.** Figure 9 shows the plots of  $([\text{CD}]\cdot[\text{BOB}])/\Delta A$  versus  $([\text{CD}] + [\text{BOB}])$ . The initial concentration of BOB is kept at  $5.0 \times 10^{-5} \text{ mol}\cdot\text{dm}^{-3}$ , while the concentrations of  $\beta$ -CD and its two derivatives are in the range from 0.0 to  $5.0 \times 10^{-3} \text{ mol}\cdot\text{dm}^{-3}$ . A linear least-squares fits to the plots. As can be seen, the fits to the plots are all excellent, with the correlation coefficients of more than 0.990. The  $K$  values of inclusion complexes of CDs with the fanlike guests are determined by the slopes and intercepts of the linear plots based on the equation shown in the experimental section. For the other nine inclusion systems, the dependencies are also linear in the investigated concentration range, further confirming that the stoichiometries of the inclusion complexes in solution are 1:1.<sup>17,23</sup>

The calculated  $K$  values of the 12 inclusion complexes are summarized in Table 4. It is interesting to speculate on the possible implications of the observed binding abilities of CDs to the fanlike guests.

First, the binding ability of  $\beta$ -CD to the four fanlike guests is lower than that of its two derivatives. This result indicates that the substitution of one methyl group or one hydroxypropyl group for the hydrogen atom on one 2-OH group can strengthen the association between the host and guest molecules.

**TABLE 4.** Calculated  $K$  Values of the 12 Inclusion Complexes at 298 K in Solution

guest	$K$ ( $\text{mol}\cdot\text{dm}^{-3}$ )		
	$\beta$ -CD	M $\beta$ -CD	HP $\beta$ -CD
EOB	$145.8 \pm 7.2$	$154.9 \pm 8.1$	$253.4 \pm 10.1$
BOB	$373.6 \pm 17.6$	$619.7 \pm 34.1$	$586.2 \pm 17.7$
DOB	$3613.5 \pm 72.3$	$5158.4 \pm 148.3$	$4340.6 \pm 106.3$
DOMB	$4890.2 \pm 68.5$	$5880.2 \pm 126.2$	$7180.7 \pm 86.2$

Second, the association ability of DOMB with the CDs is obviously higher than that of DOB, which means a positive effect of introduction of an extra methoxy group at the *ortho* position of the ether-oxygen bond of the phenyl ring on complexation.

Third, the  $K$  values of the inclusion complexes of the same CD with the guests increase in the order  $\text{EOB} < \text{BOB} \ll \text{DOB}$ . That is to say, the stability of the CD inclusion complexes of DOB or DOMB with a long chain is almost 10-fold that of the inclusion complexes of the same CD and EOB or BOB with a short chain. The finding shows the contribution of the alkyl chain of the fanlike guests to the binding affinity between host and guest molecules. According to the results described in Tables 1–4, we can presume that during the inclusion complexations between the CDs and the fanlike guests, both the benzene ring plane like a fan face and the carbon chain like a fan handle are simultaneously accommodated in the cavity of a CD molecule. Such an inclusion behavior (see Figure 5B) effectively increases the intermolecular interaction so as to improve the stabilities of the complexes.

The sequence results obtained from UV–vis spectroscopic measurements are in good accordance with those of both PM3 calculation and  $^1\text{H}$  NMR titration experiment. In order to further estimate the effect of the alkyl chain on the benzene ring of the guests on their association behaviors with  $\beta$ -CD, it is necessary to prepare and characterize the solid inclusion complexes of  $\beta$ -CD with the guests.

**Preparation Analysis of Solid Inclusion Complexes.** Two solid  $\beta$ -CD inclusion complexes, EOB- $\beta$ -CD and DOB- $\beta$ -CD, were prepared as described in the experimental section.

The results of elemental analyses: EOB- $\beta$ -CD, Anal. Calcd for  $\text{C}_{50}\text{H}_{80}\text{O}_{36}\cdot 2\text{H}_2\text{O}$ : C, 46.86; H, 6.63. Found: C, 46.61; H, 6.76; DOB- $\beta$ -CD, Anal. Calcd for  $\text{C}_{60}\text{H}_{100}\text{O}_{36}\cdot 5\text{H}_2\text{O}$ : C, 48.45; H, 7.45. Found: C, 48.44; H, 7.41. Therefore, the binding stoichiometries of  $\beta$ -CD to EOB and DOB in the two solid complexes are 1:1.

The yields of the two complexes were calculated on the basis of the initial concentration of  $\beta$ -CD. EOB- $\beta$ -CD has a yield of 45.6% in contradistinction to the value of 23.9% for DOB- $\beta$ -CD under the same dry conditions.

**IR, XRD, and ESI-MS Analyses of the Solid Inclusion Complexes.** FT-IR data of  $\beta$ -CD and its two inclusion complexes are listed in Table 5. The free  $\beta$ -CD shows strong absorption bands at 3417.6 and 1028.7  $\text{cm}^{-1}$ , attributing to  $\nu_{\text{OH}}$  and  $\nu_{\text{C-O}}$  vibrations. There are a series of peaks at 820–1180  $\text{cm}^{-1}$ , which are assigned to the  $\nu_{\text{C-O}}$  and  $\nu_{\text{C-C}}$  vibrations in the fingerprint region. FT-IR spectrum of EOB displays two sharp peaks at 1600.5 and 1496.9  $\text{cm}^{-1}$ , corresponding to the  $\nu_{\text{C=C}}$  vibration in the aromatic ring, and two strong peaks at 1244.9 and 1047.56  $\text{cm}^{-1}$  due to  $\nu_{\text{C-O}}$  vibration. DOB has IR peaks at 1650.3 and 1461.6  $\text{cm}^{-1}$  resulting from the  $\nu_{\text{C=C}}$  vibration of aromatic region. The peaks at 1109.5 and 1042.3  $\text{cm}^{-1}$  are assigned to  $\nu_{\text{C-O}}$  vibration.

(23) Cao, Y. J.; Xiao, X. H.; Lu, R. H.; Guo, Q. X. *J. Mol. Struct.* **2003**, *660*, 73–80.



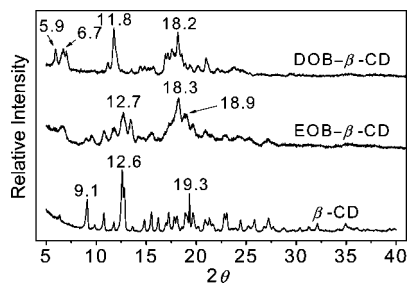


FIGURE 10. XRD spectra of  $\beta$ -CD, EOB- $\beta$ -CD, and DOB- $\beta$ -CD.

TABLE 5. FT-IR and XRD Data of  $\beta$ -CD and Its Two Complexes

	FT-IR $\nu_{C-O}$ ( $\text{cm}^{-1}$ )		
	$\beta$ -CD	EOB- $\beta$ -CD	DOB- $\beta$ -CD
	1028.7	1030.7	1025.8
	1079.8	1079.4	1156.3
	1157.4	1155.9	1180.1
peak	XRD $2\theta$ (deg)		
	$\beta$ -CD	EOB- $\beta$ -CD	DOB- $\beta$ -CD
$I_1$	12.6	18.3	11.8
$I_2$	19.3	12.7	18.2
$I_3$	9.1	18.9	5.9, 6.7

Three narrow, strong, carbon single-bonded oxygen (C–O) stretching vibrations of  $\beta$ -CD appear at 1028.7, 1079.8, and 1157.4  $\text{cm}^{-1}$ .<sup>9</sup> Upon inclusion, the characteristic vibration bands will be slightly shifted to 1030.7, 1079.4, and 1155.9  $\text{cm}^{-1}$  in EOB- $\beta$ -CD and to 1025.8, 1180.1, and 1156.3  $\text{cm}^{-1}$  in DOB- $\beta$ -CD. Similarly, the vibration bands due to EOB and DOB also present small shifts after inclusion.

Such small differences in the IR bands of  $\beta$ -CD, EOB, and DOB between values before and after inclusion are ascribed to the fact that there are no chemical bonds formed between the host and guest molecules.

The XRD patterns of  $\beta$ -CD and its inclusion complexes with EOB and DOB are shown in Figure 10. The  $2\theta$  values of the top three peaks of each curve in Figure 10 are listed in Table 5.  $I_1$  denotes the first strongest peak,  $I_2$  the second, and  $I_3$  the third. EOB and DOB are liquid at room temperature, so there are no XRD data available.

Figure 10 indicates that the  $I_1$ ,  $I_2$ , and  $I_3$  in free  $\beta$ -CD are located at  $2\theta$  values of 12.6°, 19.3°, and 9.1°,<sup>17</sup> but they appear at 18.3°, 18.9°, and 12.7° in EOB- $\beta$ -CD, and 5.9°, and 6.7° in DOB- $\beta$ -CD. Hence, there are clear differences among the XRD patterns of  $\beta$ -CD and its two complexes.

First, free  $\beta$ -CD in the low angle range of 5.0–10.0° has a strong sharp peak and a very weak peak at  $2\theta$  values of 9.1° ( $I_3$ ) and 6.4°, respectively. However, EOB- $\beta$ -CD has two weak peaks at 9.0° and 9.5° and a broad weak peak at 6.6°. DOB- $\beta$ -CD has only two strong peaks at 5.9° and 6.7° ( $I_3$ ). Interestingly, the peak at 9.1° in free  $\beta$ -CD disappears completely in DOB- $\beta$ -CD.

Second, free  $\beta$ -CD has the strongest peak at 12.6° ( $I_1$ ), but the peak is shifted to lower  $2\theta$  value for DOB- $\beta$ -CD ( $I_1$ , 11.8°) because of the enlarged lattice spacings of the complex. As is expected, this reveals that, due to the existence of the long alkyl chain on the benzene ring, DOB cannot be fully accommodated in the cavity of  $\beta$ -CD, and thus the complex gets longer than  $\beta$ -CD in the direction of the cavities. In the case of EOB- $\beta$ -CD, the peak due to the free  $\beta$ -CD (12.6°) is changed into two

peaks at 12.7° ( $I_3$ ) and 13.5°, and the intensities of the peaks rapidly decrease, indicating a more amorphous character in the complex.

Third, the strong sharp peak at 19.3° ( $I_2$ ) in free  $\beta$ -CD is obviously shifted to a lower  $2\theta$  value in EOB- $\beta$ -CD (18.3°,  $I_1$ ) and in DOB- $\beta$ -CD (18.2°,  $I_2$ ). In addition, the diffraction peak of  $\beta$ -CD becomes wider after inclusion.

The above results suggest that there is an intermolecular interaction in solid state between  $\beta$ -CD and the two guests. What is more, the remarkable differences between the diffraction patterns of EOB- $\beta$ -CD and DOB- $\beta$ -CD reflect that the effect of the chain length of the guests on their interactions with  $\beta$ -CD.

ESI-MS is a useful technique to examine the formation and composition of an inclusion complex. As an example, Figure 11 depicts the ESI-MS spectrum of EOB- $\beta$ -CD in the range of  $m/z$  from 1185 to 1445. It exhibits three peaks at  $m/z$  values of 1187.0, 1253.9, and 1432.8 due to  $\beta$ -CD $\cdot$ 2H<sub>2</sub>O, EOB- $\beta$ -CD, and EOB- $\beta$ -CD $\cdot$ 10H<sub>2</sub>O, respectively. The result confirms the quantitative formation of the 1:1 inclusion complex between EOB and  $\beta$ -CD even in the case of ESI experiments.

It can be noted from Table 6 that no peaks at around  $m/z$  of 1396 due to DOB- $\beta$ -CD are observed in its spectrum, except the reflections corresponding to two hydrates ( $\beta$ -CD $\cdot$ 3H<sub>2</sub>O and DOB- $\beta$ -CD $\cdot$ 2H<sub>2</sub>O).

The results indicate that under the ESI-MS conditions the  $\beta$ -CD complexes of the two guests with the same aromatic ring but different carbon chain lengths have different stabilities but the same host-guest stoichiometry.

**<sup>1</sup>H NMR Spectral Analysis of the Obtained Solid Inclusion Complexes in Solution.** The  $\Delta\delta$  values of the protons in  $\beta$ -CD, EOB, and DOB between free and complexed forms in DMSO-*d*<sub>6</sub> are listed in Table 7. As an example, Figure 12 displays the <sup>1</sup>H NMR spectrum of DOB- $\beta$ -CD in DMSO-*d*<sub>6</sub>.

First, the formations and chemical compositions of the inclusion complexes are further confirmed by comparing the relative integral areas of the proton signals between  $\beta$ -CD and the guest molecules. For example, the <sup>1</sup>H NMR spectrum of DOB- $\beta$ -CD in Figure 12 reveals that the stoichiometry of DOB binding to the  $\beta$ -CD receptor is 1:1. This is a good agreement with the result of elemental analysis.

Second, the proton signals of H-3 and H-5 inside  $\beta$ -CD cavity are shifted upfield in the complexes. As shown in Table 7, the signals of H-3 and H-5 are more affected than those of H-2 and H-4 outside the cavity of  $\beta$ -CD, suggesting that the guests have penetrated into the cavity. This observation is confirmed by the fact that upon complexation the proton signals of EOB and DOB are to some extent shifted upfield. Further, the protons due to the aromatic ring (H-a and H-b) and methylene (H-c) of DOB have a larger  $\Delta\delta$  value than those of its end methyl group in DOB- $\beta$ -CD, suggesting that the aromatic ring is located inside the cavity.

Third, the proton signals of H-3, located close to the wider rim of the cavity, are less shifted in comparison with those of H-5, located close to the other rim of the cavity, indicating that the interaction between the guests and  $\beta$ -CD takes place in the region from the center to the small opening of the cavity.

Figure 13A is the <sup>1</sup>H NMR spectrum of the physical mixture (1:28, molar ratio) of DOB with a large excess of 1-bromododecane. Figure 13B is the <sup>1</sup>H NMR spectrum of the product formed by  $\beta$ -CD with the mixture, which was prepared using the method described in the Experimental Section. Although the composition of the two guests in the mixture is distinct,

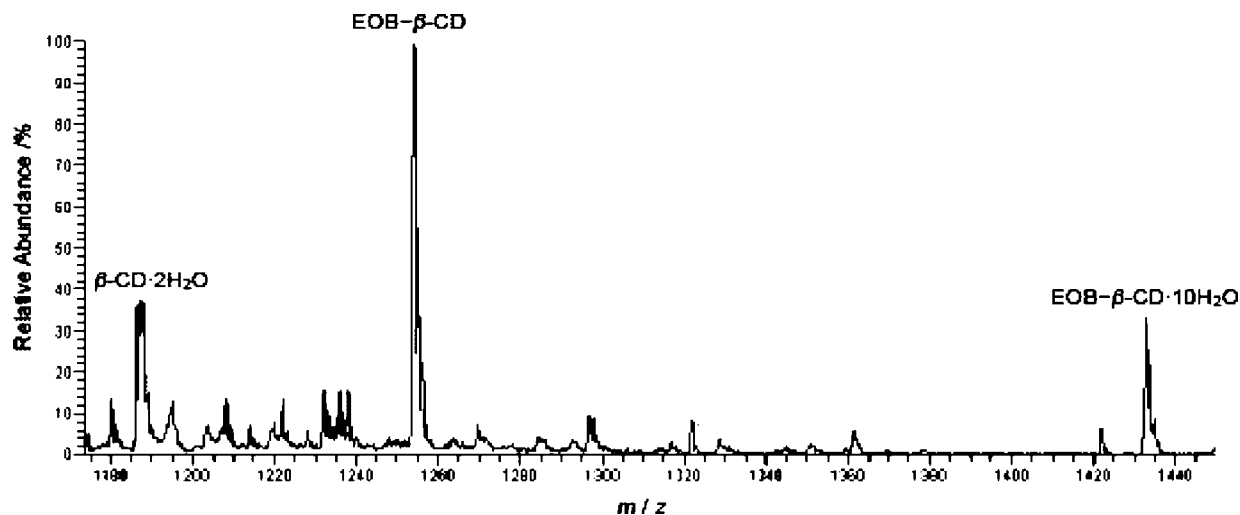


FIGURE 11. ESI-MS spectrum of EOB- $\beta$ -CD.

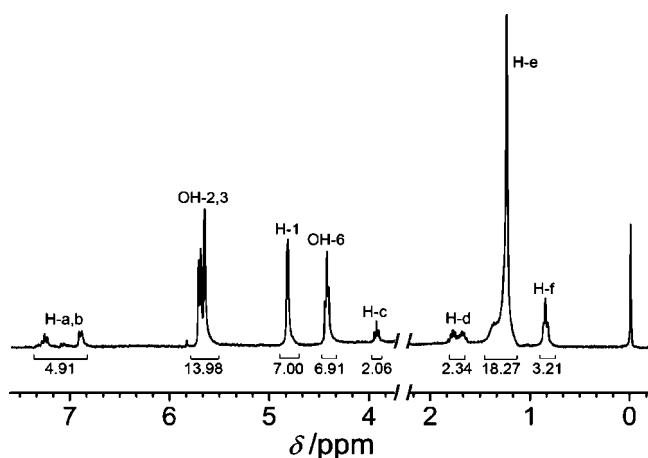


FIGURE 12.  $^1\text{H}$  NMR spectrum (300 MHz,  $\text{DMSO}-d_6$ , 298 K) of the inclusion complex of  $\beta$ -CD with DOB.

TABLE 6. ESI-MS Data of EOB- $\beta$ -CD and DOB- $\beta$ -CD

complex	ESI-MS	
	$m/z$	composition
$\beta$ -CD-EOB	1187.0	$\text{C}_{42}\text{H}_{70}\text{O}_{35}\cdot 3\text{H}_2\text{O}$
	1253.9	$\text{C}_{42}\text{H}_{70}\text{O}_{35}\cdot \text{C}_8\text{H}_{10}\text{O}$
	1432.8	$\text{C}_{42}\text{H}_{70}\text{O}_{35}\cdot \text{C}_8\text{H}_{10}\text{O}\cdot 10\text{H}_2\text{O}$
$\beta$ -CD-DOB	1187.0	$\text{C}_{42}\text{H}_{70}\text{O}_{35}\cdot 3\text{H}_2\text{O}$
	1432.0	$\text{C}_{42}\text{H}_{70}\text{O}_{35}\cdot \text{C}_{18}\text{H}_{30}\text{O}\cdot 2\text{H}_2\text{O}$

TABLE 7.  $\Delta\delta$  (ppm) Values of the Protons in  $\beta$ -CD, EOB, and DOB between Free and Complexed Forms

proton	$\beta$ -CD		proton	$\Delta\delta_{\beta\text{-CD}}$	
	$\Delta\delta_{\text{EOB}}$	$\Delta\delta_{\text{DOB}}$		EOB	DOB
H-1	0.012	0.014	H-a	0.013	-0.029
H-2	0.021	0.026	H-b	0.018	-0.026
H-3	-0.028	-0.034	H-c	0.025	-0.021
H-4	0.024	0.026	H-d	-0.015	-0.023
H-5	-0.051	-0.052	H-e		-0.014
H-6	0.012	0.008	H-f		-0.012

upon complexation their proportions in the product are approximately the same based on the relative integral intensities of the signals in the  $^1\text{H}$  NMR spectrum of their  $\beta$ -CD complexes. Hence, even if there exists a competitive complexation between DOB and 1-bromododecane for  $\beta$ -CD, in general we can

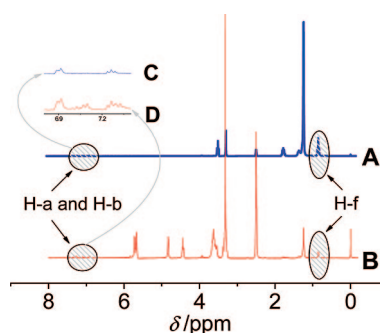


FIGURE 13.  $^1\text{H}$  NMR spectra (300 MHz,  $\text{DMSO}-d_6$ , 298 K): (A) the physical mixture (1:28, molar ratio) of DOB and 1-bromododecane and (B) their complexes of  $\beta$ -CD. The insets (C and D) are the magnification of the spectra (A and B) ranging from 6.8 to 7.4 ppm.

conclude that the DOB molecule with an aromatic ring prefers to be bound noncovalently to the cavity of  $\beta$ -CD.

As shown in Figure 14, several cross-peaks related to spatial interactions between the aromatic and aliphatic protons of DOB and the inside-cavity protons of  $\beta$ -CD clearly appears. For example, the NOE cross-peaks (peaks A) between H-3/H-5 protons of  $\beta$ -CD cavity and H-a/H-b protons are observed, suggesting that the benzene ring of DOB is included into the  $\beta$ -CD cavity. Meantime, the NOE cross-peaks between H-d/H-e protons of the aliphatic chain and H-3/H-5 of the  $\beta$ -CD cavity are also observed (peaks B and C), indicating that the aliphatic moiety of DOB also has interactions with the inside-cavity protons of  $\beta$ -CD, i.e., the aliphatic carbon chain of DOB is partly inserted in the cavity of  $\beta$ -CD.

Furthermore, a cross-peak (peak D) between the H-b protons of the benzene ring and H-c protons of DOB is also clearly observed, confirming that the long carbon chain in DOB is in a folded position. Based on the results discussed above, we thus conclude that both the aromatic and aliphatic moieties of DOB are synchronously included into the  $\beta$ -CD cavity. This conclusion is just in good accordance with the results of theoretical PM3 calculation.

**Differences in TG Profiles between Free  $\beta$ -CD and Its Two Inclusion Complexes.** The TG curves of free  $\beta$ -CD, EOB- $\beta$ -CD and DOB- $\beta$ -CD at a constant heating rate of  $5\text{ K}\cdot\text{min}^{-1}$  are shown in Figure 15. Obviously, the shapes of the three TG curves are quite different from one another. In order to conveniently make a direct comparison, the thermal decom-



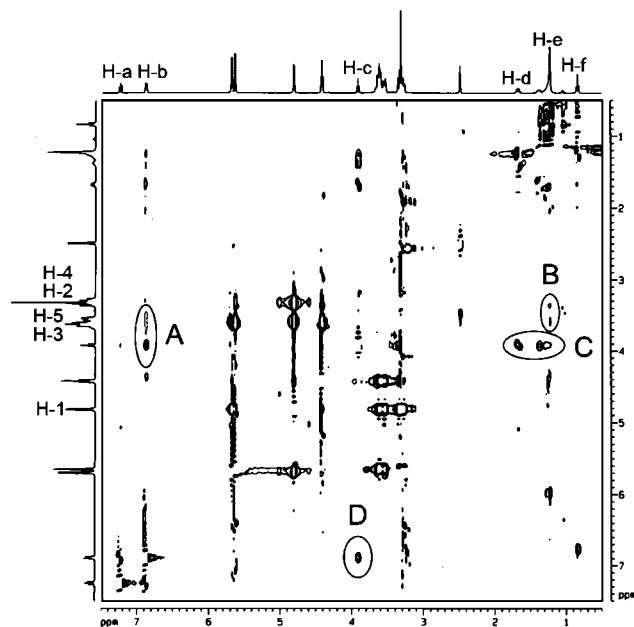


FIGURE 14. ROESY spectrum of DOB- $\beta$ -CD with a mixing time of 200 ms at 300 K.

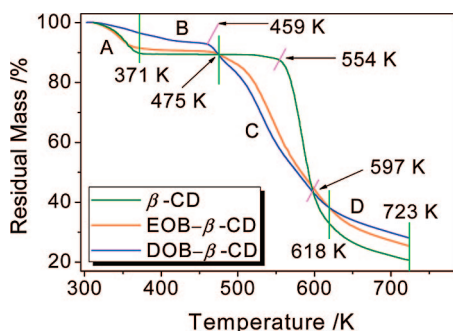


FIGURE 15. TG profiles of free  $\beta$ -CD, EOB- $\beta$ -CD, and DOB- $\beta$ -CD at the heating rate of  $5.0 \text{ K} \cdot \text{min}^{-1}$ .

position processes of the three samples in the range from 300 to 723 K are roughly divided into four steps (A–D) using green lines in Figure 15.

Free EOB and DOB are both liquid, but they are solidified in the presence of  $\beta$ -CD at room temperature. Because of the low melting points and high boiling points, the guests in their complexes of  $\beta$ -CD will melt and volatilize with increasing temperature. As would be expected, in the range of Step A from room temperature to about 371 K, free  $\beta$ -CD loses its water molecules. The two complexes lose their respective water molecules, and the guests in the complexes melt and volatilize. The step for free  $\beta$ -CD or EOB- $\beta$ -CD is sharper than that for DOB- $\beta$ -CD. This is because the boiling point of DOB with a big molecular mass is much higher than that of EOB with a low molecular mass.

In Step B, free  $\beta$ -CD almost completely does not lose its mass, and EOB- $\beta$ -CD has a very slow small mass loss. However, DOB- $\beta$ -CD shows an obvious mass loss, and the rate of the loss is accelerated at 459 K. The three curves intersect at a point whose abscissa is equal to 475 K. Before 475 K of the stage the residual mass of  $\beta$ -CD is slightly lower than that of EOB- $\beta$ -CD but obviously lower than that of DOB- $\beta$ -CD. The observations can be explained by the high boiling point of DOB.

In the range of Step C from 475 to 618 K, the two inclusion complexes begin to decompose rapidly. Differently,  $\beta$ -CD has a very slow small mass loss at the beginning of the region and begins to lose its mass sharply at a higher temperature of 554 K. Since the molecular mass of  $\beta$ -CD is much higher than those of the two guests, the results indicate that the existence of the fanlike guest molecules leads to advanced decomposition of  $\beta$ -CD possibly because the intermolecular interaction between  $\beta$ -CD and the guests is weaker than that between the  $\beta$ -CD molecules. And then, the three curves almost intersect at a point at about 597 K again. During the temperature range of about 475–597 K the residual masses of the two complexes are considerably lower than that of  $\beta$ -CD.

In Step D, free  $\beta$ -CD, EOB- $\beta$ -CD and DOB- $\beta$ -CD begin to further decompose, but their decomposition rates obviously decrease, especially that of free  $\beta$ -CD when compared with in Step C. During the stage, the residual masses of the two complexes are markedly higher than that of free  $\beta$ -CD. For example, the residual masses of free  $\beta$ -CD, EOB- $\beta$ -CD and DOB- $\beta$ -CD are 21%, 26% and 28% at 723 K (see Figure 15). The finding demonstrates that the fanlike guests can dramatically retard the thermal decomposition of  $\beta$ -CD at the high temperature range from 597 to 700 K.

**Similarities in Thermal Decomposition Kinetics of the Two Solid Inclusion Complexes.** The TG profiles of EOB- $\beta$ -CD and DOB- $\beta$ -CD at heating rates of 5, 10, 15, 20, and 25  $\text{K} \cdot \text{min}^{-1}$  ( $\zeta_1$ – $\zeta_5$ ) are depicted in Figure 16A and B, respectively.

The thermal decomposition processes of the two inclusion complexes can be divided into three consecutive stages, i.e., a slow stage, a rapid stage and a moderate stage. The kinetics of the thermal decomposition process of an inclusion complex can be described as follows:

$$\frac{d\alpha}{dt} = k f(\alpha) = A \exp\left(\frac{-E_a}{RT}\right) f(\alpha) \quad (2)$$

where  $\alpha$  is the fraction of the inclusion complex that undergoes decomposition at the heating time  $t$ ,  $f(\alpha)$  is a function of ( $\alpha$ ), and  $k$ ,  $A$ ,  $E_a$ ,  $R$ , and  $T$  are the rate constant, pre-exponential factor, activation energy, molar gas constant, and absolute temperature of the degradation process of the inclusion complex, respectively.

Through a series of mathematical treatments, eq 2 can be changed into the following form, i.e., the so-called Flynn–Wall–Ozawa (FWO) equation:<sup>24</sup>

$$\ln \zeta = \ln\left(\frac{AE_a}{R}\right) - 5.3305 - 1.0516 \frac{E_a}{RT} - \ln F(\alpha) \quad (3)$$

where  $F(\alpha)$  is a power series expansion for the integration of the exponential term of eq 2. So, for a constant degree of conversion, the plot of  $\ln \zeta$  versus  $1/T$  should theoretically result in a straight line, whose slope is approximately  $-1.0516E_a/R$ .

As shown in Figure 17, there exists a very good linear correlation between  $\ln \zeta$  and  $1/T$ . The correlation coefficient ( $r$ ) values of the linear fit lines of EOB- $\beta$ -CD and DOB- $\beta$ -CD are in the range from 0.984 to 0.990 and from 0.992 to 0.999, respectively.

According to the slopes of the straight lines in Figure 17, the  $E_a$  values of the decomposition processes of the inclusion complexes at different mass losses are calculated. The average values of  $E_a$  for EOB- $\beta$ -CD and DOB- $\beta$ -CD are  $122.34 \pm$

(24) Popescu, C. *Thermochim. Acta* **1996**, *285*, 309–323.

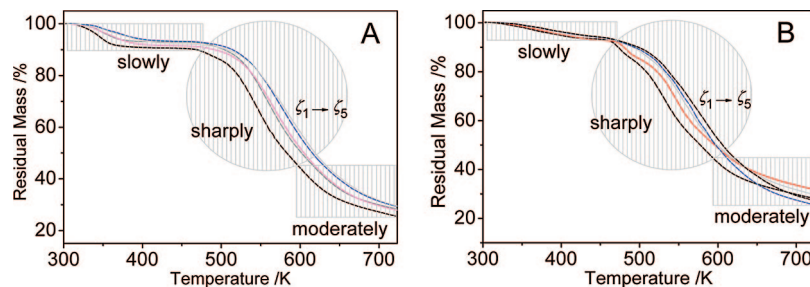


FIGURE 16. TG profiles of EOB- $\beta$ -CD (A) and DOB- $\beta$ -CD (B) at heating rates of 5, 10, 15, 20 and 25  $\text{K}\cdot\text{min}^{-1}$  ( $\zeta_1$ – $\zeta_5$ ).

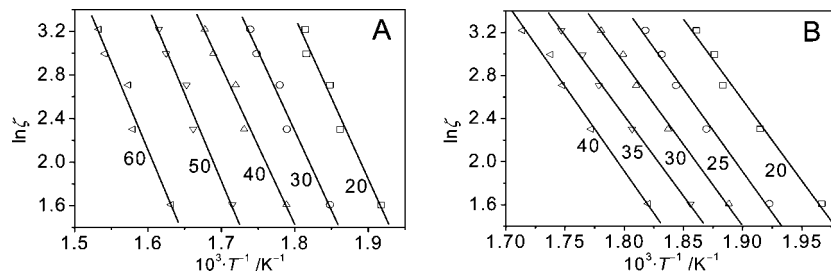


FIGURE 17. FWO plots of the  $\beta$ -CD inclusion complexes of EOB (A) and DOB (B).

11.10 and  $120.74 \pm 6.41 \text{ kJ}\cdot\text{mol}^{-1}$ , respectively, which are significantly larger than the average  $E_a$  value of  $86.2 \text{ kJ}\cdot\text{mol}^{-1}$  of free  $\beta$ -CD<sup>25</sup> according to the same method. The finding demonstrates that the thermal decomposition behaviors of the survived  $\beta$ -CD in an inclusion complex are influenced by the released guest molecules.<sup>26,27</sup> This influence is realized through the change of intermolecular interaction between  $\beta$ -CD molecules because of the existence of guests.<sup>26</sup>

There is only a slight difference between the average  $E_a$  values of EOB- $\beta$ -CD and DOB- $\beta$ -CD. The result suggests that the large difference in the TG profiles between two inclusion complexes is not consequentially associated with the large difference in the kinetics of their thermal decomposition processes.

## Conclusion

The results of theoretical and experimental studies in the present work show a significant relationship between the side chain length of the substituent on the aromatic ring of the fanlike guests and the binding abilities of CDs to the guests. That is to say, the aromatic guests with a longer fan handle, such as DOB and DOMB, have much stronger interactions with the CDs when compared with those with a short fan handle, such as EOB and BOB. Also, the structural transformation of side chains from an extended form to a folded form leads to a positive contribution to the inclusion complexation between host and guest. The binding mode of a side chain unit that is held in a folded position by the CD cavity could be very useful for site-selective reactions in organic synthesis. Even a minor structural modification on the 2-OH group of one of seven glucose units of the host  $\beta$ -CD as well as on the benzene ring of the guest DOB can make a large difference in terms of both decreasing  $\Delta E_i$  and increasing  $K$ . It is hoped that further research will be continued, so that data obtained from experimental work will

provide a better understanding of what kinds of combinations between a selected aromatic ring unit and an appropriate side chain of organic guests are most likely to promote the formation and stability of CD inclusion complexes of the guests.

## Experimental Section

**Materials.**  $\beta$ -CD was recrystallized twice from deionized water.  $M\beta$ -CD,  $HP\beta$ -CD, 1-bromoethane, 1-bromobutane, and 1-bromododecane were used without further purification. All reagents are of analytical reagent grade, unless stated otherwise.

**Instruments.** Elemental analyses were carried out on an elemental analyzer. TG curves were recorded on a thermogravimetric analyzer at constant heating rates of 5 ( $\zeta_1$ ), 10 ( $\zeta_2$ ), 15 ( $\zeta_3$ ), 20 ( $\zeta_4$ ), and 25  $\text{K}\cdot\text{min}^{-1}$  ( $\zeta_5$ ) under a nitrogen atmosphere with gas flow of  $25 \text{ mL}\cdot\text{min}^{-1}$ . The TG plot of free  $\beta$ -CD was recorded at the heating rate of 5  $\text{K}\cdot\text{min}^{-1}$ . In the current case approximately 10 mg of a solid sample as crystalline powder was used in an alumina crucible every time. XRD analyses of the solid complexes were performed on a X-ray diffractometer. The samples were irradiated with monochromatized  $\text{Cu K}\alpha$  and analyzed with  $5^\circ \leq 2\theta \leq 40^\circ$ . Tube voltage and current were 40 kV and 40 mA, respectively. FTIR transmission spectroscopy measurements were taken with a spectrometer in KBr discs in the range of 4000–400  $\text{cm}^{-1}$ . ESI-MS analysis was performed on an LTQ linear ion trap mass spectrometer. The interface was operated at positive ion mode at a spray voltage of 5000 V, capillary voltage of 16 V, and capillary temperature of 548 K. Electronic spectroscopy of aqueous samples of guest molecules, with and without  $\beta$ -,  $M\beta$ -, and  $HP\beta$ -CD were performed on a UV-vis recording spectrophotometer over the wavelength range between 200 and 800 nm, using quartz cells with a 1 cm optical path at room temperature.  $^1\text{H}$  NMR spectra of two solid complexes, EOB- $\beta$ -CD and DOB- $\beta$ -CD, were obtained on a NMR spectrometer at 300 MHz at 298 K using  $\text{DMSO-}d_6$  as solvent.

**General Procedure for the Preparation and Characterization of EOB, BOB, DOB, and DOMB.** EOB was synthesized according to a similar method described in the literature.<sup>28</sup> After being dried with anhydrous sodium sulfate and removal of the solvent in a vacuum, it was separated by distillation to give EOB, a colorless

(25) Song, L. X.; Teng, C. F.; Xu, P.; Wang, H. M.; Zhang, Z. Q.; Liu, Q. Q. *J. Inclusion Phenom. Macrocyclic Chem.* **2008**, *60*, 223–233.

(26) Xu, P.; Song, L. X.; Wang, H. M. *Thermochim. Acta* **2008**, *469*, 36–42.

(27) Xu, P.; Song, L. X. *Acta Phys.-Chim. Sin.* **2008**, *24*, 729–736.

(28) McKillop, A.; Fiaud, J. C.; Hug, R. P. *Tetrahedron* **1974**, *30*, 1379–1382.

liquid (2.06 g, 84.3%), bp 169 °C.  $^1\text{H NMR}$  (300 MHz,  $\text{CDCl}_3$ )  $\delta_{\text{H}}$  7.21–7.26 (2H, m, aromatic H), 6.85–6.92 (3H, m, aromatic H), 3.95 (2H, q,  $J$  7.0 Hz,  $\text{OCH}_2$ ), 1.37 (3H, t,  $J$  7.2 Hz,  $\text{CH}_2\text{CH}_3$ );  $^{13}\text{C NMR}$  (75 MHz,  $\text{CDCl}_3$ )  $\delta_{\text{C}}$  159.1, 129.5, 120.6, 114.6, 63.3, 14.9.

By means of the method described above, BOB and DOB were obtained as colorless liquids. The yields of BOB and DOB were 86.4% and 77.3%, respectively. BOB, bp 210 °C,  $^1\text{H NMR}$  (300 MHz,  $\text{CDCl}_3$ )  $\delta_{\text{H}}$  7.21–7.26 (2H, m, aromatic H), 6.85–6.91 (3H, m, aromatic H), 3.91 (2H, q,  $J$  6.3 Hz,  $\text{OCH}_2$ ), 1.75 (2H, dq,  $J_1$  6.6 Hz,  $J_2$  6.7 Hz,  $\text{OCH}_2\text{CH}_2$ ), 1.51 (2H, m, 2H,  $\text{OCH}_2\text{CH}_2\text{CH}_2$ ), 0.96 (3H, t,  $J$  7.2 Hz,  $\text{CH}_2\text{CH}_3$ );  $^{13}\text{C NMR}$  (75 MHz,  $\text{CDCl}_3$ )  $\delta_{\text{C}}$  159.3, 129.4, 120.5, 114.6, 67.6, 31.5, 19.4, 13.9. DOB, bp 197 °C (12 torr),  $^1\text{H NMR}$  (300 MHz,  $\text{CDCl}_3$ )  $\delta_{\text{H}}$  7.25–7.33 (2H, m, aromatic H), 6.87–6.96 (3H, m, aromatic H), 3.95 (2H, t,  $J$  6.6 Hz,  $\text{OCH}_2$ ), 1.80 (2H, dq,  $J_1$  6.7 Hz,  $J_2$  6.7 Hz,  $\text{OCH}_2\text{CH}_2$ ), 1.25–1.50 [18H, m,  $\text{OCH}_2\text{CH}_2(\text{CH}_2)_9$ ], 0.88 (3H, t,  $J$  6.6 Hz,  $\text{CH}_2\text{CH}_3$ );  $^{13}\text{C NMR}$  (75 MHz,  $\text{CDCl}_3$ )  $\delta_{\text{C}}$  159.1, 129.4, 120.4, 114.4, 67.8, 31.9, 29.34, 29.26, 26.0, 22.7, 14.1.

DOMB was prepared and purified by a previous method.<sup>29</sup> After the reaction was finished, the product, in the form of finely divided crystals, was filtered, washed with water (50.0 mL), extracted with dichloromethane ( $2 \times 50.0$  mL), and concentrated in vacuo to give the essentially pure DOMB as an acicular crystal (6.93 g, 79.0%), mp 47 °C.  $^1\text{H NMR}$  (300 MHz,  $\text{CDCl}_3$ )  $\delta_{\text{H}}$  6.89 (4H, s, aromatic H), 4.01 (2H, t,  $J$  6.9,  $\text{OCH}_2$ ), 3.86 (3H, s,  $\text{OCH}_3$ ), 1.84 (2H, m,  $\text{OCH}_2\text{CH}_2$ ), 1.26–1.55 (18H, m,  $\text{OCH}_2\text{CH}_2(\text{CH}_2)_9$ ), 0.88 (3H, t,  $J$  6.6,  $\text{CH}_2\text{CH}_3$ );  $^{13}\text{C NMR}$  (75 MHz,  $\text{CDCl}_3$ )  $\delta_{\text{C}}$  150.3, 121.2, 110.8, 68.9, 56.3, 31.7, 29.7, 26.0, 22.6, 14.1.

**Theoretical Studies of the Inclusion Complexations between CDs and the Four Fanlike Guests.** PM3 method implemented in the MOPAC<sup>30</sup> software package was chosen to investigate the inclusion complexation between three CD molecules and four guest molecules in water. The initial geometry of  $\beta$ -CD was constructed on the basis of available crystallographic data<sup>31</sup> and fully optimized without any restrictions. The coordinates of M $\beta$ - and HP $\beta$ -CD were obtained with the help of GaussView software, by substituting the C-2 OH group of one glucopyranose unit in  $\beta$ -CD with a methoxy group and a hydroxypropyloxy group, respectively. The geometries of the four guest molecules were also fully optimized. The optimum positions of complex formation were determined by trying several starting points rather than by a global search.<sup>9,32–35</sup>

The complexation energy ( $\Delta E_c$ ) between CD and a guest molecule is the difference between the energy of the inclusion complex at the lowest energy configuration and the sum of energies of CD and the guest in their respective optimized equilibrium geometry.<sup>17,36</sup> The deformation energy ( $\Delta E_d$ ) is the difference between the sums of energies of two partners of an inclusion complex at their respective equilibrium geometries and at the geometry in the complex.<sup>17,36</sup> Interaction energy ( $\Delta E_i$ ) is the difference between the energy of the complex at the lowest-energy configuration and the sum of the energies of both partners at the geometry of the complex.<sup>17,37,38</sup> Accordingly, the interaction energy

between a guest and CD can be calculated as the sum of the complexation energy and the deformation energies of CD and the guest.<sup>17,38,39</sup>

**Preparation of Solutions in UV–vis Absorption Spectroscopy Measurements of the Inclusion Systems between CDs and the Four Fanlike Guests.** Stock solutions of guests were prepared by dissolving the guest compounds in water–ethanol (3:1, v:v). On the basis of our observation, the four guests were soluble in the mixed solvent. In UV–vis spectroscopy measurements, all analyte solutions were freshly prepared by dilution of stock solutions. The concentrations of the guests in sample solutions were kept constant at  $5.0 \times 10^{-5} \text{ mol}\cdot\text{dm}^{-3}$ , while the concentration of CD varied between 0 to  $5.0 \times 10^{-3} \text{ mol}\cdot\text{dm}^{-3}$  in order to determine the binding constants of CD to the guests. All sample solutions to be detected were prepared by mixing CD with a guest in water–ethanol (3:1, v:v) before use and kept stirring at 298 K for 30 min.

**Determination of Chemical Stoichiometries in the Inclusion Complexes of CDs and the Four Fanlike Guests in Solution.** Job's continuous variation method<sup>22,40</sup> was applied to determine the stoichiometries of the inclusion complexes of CDs with the guests. In the measurements, a series of solutions were prepared, each having a total concentration ( $[\text{CD}] + [\text{guest}]$ ) of  $1.0 \times 10^{-4} \text{ mol}\cdot\text{dm}^{-3}$  while the  $[\text{CD}]:[\text{guest}]$  ratio value increased from 0 to 1.

**Determination of Formation Constants of the Inclusion Complexes of CDs with the Fanlike Guests.** The determination of formation constants ( $K$ ) of  $\beta$ -CD and its derivatives to the guests was realized by UV–vis spectroscopy titration experiments. The  $K$  values were calculated by applying least-squares fit to the plots of  $([\text{CD}] \cdot [\text{guest}])/\Delta\epsilon$  versus  $([\text{CD}] + [\text{guest}])$ , according to the modified Benesi–Hildebrand equation:<sup>10,41</sup>

$$\frac{[\text{G}][\text{CD}]}{\Delta\epsilon} = \frac{1}{K\Delta\epsilon} + \frac{1}{\Delta\epsilon}([\text{G}] + [\text{CD}]) \quad (4)$$

In eq 4,  $[\text{G}]$  and  $[\text{CD}]$  are the equilibrium concentrations of guest and CD, respectively.  $\Delta\epsilon$  is the difference between the extinction coefficients of free and complexed guest.  $\Delta\epsilon$  is the difference between the absorbances of free and complexed guest at the same wavelength.

**$^1\text{H NMR}$  Titration Measurements of the Interaction between  $\beta$ -CD and the Four Guests.**  $^1\text{H NMR}$  titrations were performed by addition of a stock solution of the guests to a solution of  $\beta$ -CD at 298 K using  $\text{DMSO}-d_6$  as solvent. The chemical shifts of protons of  $\beta$ -CD and the guests were recorded with the concentration of the guests ranging from 0 to  $2.5 \times 10^{-1} \text{ mol}\cdot\text{dm}^{-3}$ , keeping that of  $\beta$ -CD constant ( $5.0 \times 10^{-3} \text{ mol}\cdot\text{dm}^{-3}$ ). All liquid samples before use were kept for 3 h under ultrasonic vibration at room temperature.

**2D-NMR ROESY Experiment of the Interaction between  $\beta$ -CD and DOB.** Two-dimensional rotating frame nuclear Overhauser effect spectroscopy (ROESY) experiment was carried out on a Bruker AV400 spectrometer at 400 MHz. A Bruker standard sequence was necessary to make an observation of an intermolecular nuclear Overhauser effect (NOE) between  $\beta$ -CD and DOB. The data consisted of 16 scans collected over 1024 complex points and for a spectral width of 4006 Hz. A mixing time of 200 ms, a repetition delay of 2.0 s, an acquisition time of 0.167 s, and a 90° pulse width of 12.5  $\mu\text{s}$  at 1 dB power attenuation were used. The data were zero-filled to  $2048 \times 512$  points and processed by applying a  $\pi/2$  shifted  $Q$ -sine window in both dimensions. Small cross-peaks were neglected because their magnitude was close to that of noise.

**Preparation of Solid  $\beta$ -CD Inclusion Complexes of EOB and DOB.** Solid inclusion complexes were prepared by mixing a guest with  $\beta$ -CD and stirring for 48 h at 298 K. The initial molar ratio of guest to  $\beta$ -CD (1 mmol, 1.14 g) was 10:1 in deionized water. During

(29) Boden, N.; Bushby, R. J.; Cammidge, A. N.; El-Mansoury, A.; Martin, P. S.; Lu, Z. B. *J. Mater. Chem.* **1999**, *9*, 1391–1402.

(30) Stewart, J. J. P. *J. Mol. Model.* **2007**, *13*, 1173–1213.

(31) Lindner, K.; Saenger, W. *Carbohydr. Res.* **1982**, *99*, 103–115.

(32) Li, X. S.; Liu, L.; Guo, Q. X.; Chu, S. D.; Liu, Y. C. *Chem. Phys. Lett.* **1999**, *307*, 117–120.

(33) Liu, L.; Guo, Q. X. *J. Inclusion Phenom. Macrocyclic Chem.* **2004**, *50*, 95–103.

(34) Castro, R.; Berardi, M. J.; Cordova, E.; de Olza, M. O.; Kaifer, A. E.; Evansck, J. D. *J. Am. Chem. Soc.* **1996**, *118*, 10257–10268.

(35) Yu, Y. M.; Chipot, C.; Cai, W. S.; Shao, X. G. *J. Phys. Chem. B* **2006**, *110*, 6372–6378.

(36) Piel, G.; Dive, G.; Evrard, B.; Van Hees, T.; de Hassonville, S. H.; Delattre, L. *Eur. J. Pharm. Sci.* **2001**, *13*, 271–279.

(37) Pascal, B.; Maud, G.; Georges, D.; Adelin, A.; Valery, B.; Bruno, P.; Didier, C.; Geraldine, P.; Luc, D.; Brigitte, E. *J. Pharm. Pharmaceut. Sci.* **2005**, *8*, 164–175.

(38) Wang, H. M.; Song, L. X. *Chem. Lett.* **2007**, *36*, 596–597.

(39) Klamt, A.; Schuurmann, G. *J. Chem. Soc., Perkin Trans. 2* **1993**, 799–805.

(40) Job, P. *Ann. Chim.* **1928**, *9*, 113–203.



stirring, a white precipitation was observed. After the reaction ended, the white precipitation was filtered, washed with deionized water ( $3 \times 5.0$  mL) and anhydrous ethanol ( $3 \times 3.0$  mL) and then dried under vacuum. Two solid inclusion complexes, EOB- $\beta$ -CD (yield, 45.6%) and DOB- $\beta$ -CD (yield, 23.9%), were obtained in this manner and stored in a vacuum desiccator over silica gel until further required.

**Supporting Information Available:**  $^1\text{H}$  NMR and FTIR spectra as well as preparation and purification of guests EOB,

BOB, DOB, and DOMB; details of materials and instruments; and details of theoretical studies. This material is available free of charge via the Internet at <http://pubs.acs.org>.

JO801436H

---

(41) Benesi, H. A.; Hildebrand, J. H. *J. Am. Chem. Soc.* **1949**, *71*, 2703–2707.